PCCP

ROYAL SOCIETY OF CHEMISTRY

PAPER

View Article Online
View Journal | View Issue

Cite this: *Phys. Chem. Chem. Phys.*, 2024, **26**, 23447

Density-based quantification of steric effects: validation by Taft steric parameters from acid-catalyzed hydrolysis of esters†

Jingwen Zhang,[a] Xin He,[b] Bin Wang,[c] Chunying Rong, *[a] Dongbo Zhao *[d] and Shubin Liu *[ef]

The steric effect is one of the most widely used concepts for chemical understanding in publications and textbooks, yet a well-accepted formulation of this effect is still elusive. Experimentally, this concept was quantified by the acid-catalyzed hydrolysis of esters, yielding the so-called Taft steric parameter. Theoretically, we recently proposed a density-based scheme to quantify the effect from density functional theory. In this work, we directly compare these two schemes, one from theory and the other from experiment. To this end, we first establish the ester hydrolysis mechanism with multiple water molecules explicitly considered and then apply the energetic span model to represent the hydrolysis barrier height between the two schemes. Our results show that the barrier height of the reaction series is strongly correlated with both Taft steric parameters from experiment and steric quantification from theory. We also obtained strong correlations with steric potential, steric force, and steric charge from our theoretical scheme. Strong correlations with a few information-theoretic quantities are additionally unveiled. To the best of our knowledge, this is the first time in the literature that such a direct comparison between theoretical and experimental results is made. These results also suggest that our proposed two-water three-step mechanism for ester hydrolysis is effective, and our theoretical quantification of the steric effect is valid, robust, and experimentally comparable. In our view, this work should have satisfactorily addressed the issue of how the steric effect can be formulated and quantified, and thus it lays the groundwork for future applications.

Received 9th July 2024,
Accepted 16th August 2024

DOI: 10.1039/d4cp02702g

rsc.li/pccp

Introduction

Density functional theory (DFT)[1,2] has been widely accepted as the workhorse of electronic structure calculations for molecules and solids alike in the past few decades. Nevertheless, the endeavor to use density-based quantities from the DFT framework to enhance chemical understanding and predict chemical reactivity is still ongoing.[3,4] The pioneering work on this topic is conceptual DFT[1,5–9] by Parr and coworkers, who formulated concepts such as hardness and softness,[10–12] Fukui function,[13–15] and electrophilicity.[16,17] Other examples along the line are the ELF (electron localization function) index,[18–20] NCI (noncovalent interaction) index,[21,22] SCI (strong covalent interaction) index,[23,24] BNI (bonding and nonbonding interaction) index,[25] electrophilicity/nucleophilicity,[26–29] cooperativity/frustration,[30–36] *etc.* Bader's quantum theory of atom in molecules[37] can also be regarded to belong to this category because it employs density-based quantities such as a density gradient and Laplacian for various applications.[3,4]

Steric effects refer to the influence of the physical size and spatial arrangement of atoms or groups within a molecule on its reactivity. These effects can affect the rates of chemical reactions and the stability of intermediates. Earlier, we proposed a density-based formulation to quantify steric effects,[38] which has been one of the most widely used chemical concepts in chemistry, but for which there is no unique way to define because no physical observable is associated with this effect. We have applied this DFT formulation of steric effects to account for its impact on numerous systems and phenomena,[39–47] including conformational

[a] *College of Chemistry and Chemical Engineering, Hunan Normal University, Changsha, Hunan 410081, China. E-mail: shubin@email.unc.edu*
[b] *Institute of Frontier Chemistry, School of Chemistry and Chemical Engineering, Shandong University, Qingdao, Shandong 266237, China*
[c] *Research Group of General Chemistry (ALGC), Vrije Universiteit Brussel (VUB), Pleinlaan 2, 1050 Brussels, Belgium*
[d] *Institute of Biomedical Research, Yunnan University, Kunming 650500, Yunnan, China*
[e] *Research Computing Center, University of North Carolina, Chapel Hill NC 27599-3420, USA*
[f] *Department of Chemistry, University of North Carolina, Chapel Hill NC 27599-3290, USA*

† Electronic supplementary information (ESI) available. See DOI: https://doi.org/10.1039/d4cp02702g

stability,[41,47] anomeric effects,[39,48,49] S_N2 reactions,[40,50,51] and stereoselectivity.[51,52] On the other hand, experimentally, there exists an empirical scale using Taft steric parameters[53–59] to quantitatively gauge the effect. This experimental scale employing the acid catalyzed hydrolysis of esters was obtained by the apparent rate constant of ester hydrolysis through a linear free energy relationship with the rate of the methyl group system as the reference.[56,57] Given these two approaches to quantify the same effect, one from experiment and the other from theory, one natural question to ask is whether or not there is any correlation between the theoretical quantification and the Taft steric parameter. This question is what we will address in this work.

Methodology

Assuming that the total energy E of an electronic system comes from the contribution of three independent physicochemical effects, steric E_s, electrostatic E_e, and quantum E_q, $E \equiv E_s + E_e + E_q$, we have proved that the steric energy E_s is simply the Weizsäcker kinetic energy T_W,[38]

$$E_s \equiv T_W = \frac{1}{8}\int \frac{|\nabla\rho(r)|^2}{\rho(r)}\mathrm{d}r, \tag{1}$$

where $\rho(r)$ is the ground state electron density satisfying the normalization condition of $\int(r)\mathrm{d}r = N$, with N as the total number of electrons and $\nabla\rho$ is the density gradient. Conventionally, in DFT,[1] we have $E = T_S + V_{ne} + J + E_{xc} + V_{nn}$, where T_s, V_{ne}, J, V_{nn}, and E_{xc} stand for the total non-interacting kinetic energy, nuclear–electron attraction, classical electron–electron Coulombic repulsion, nuclear–nuclear repulsion, and exchange-correlation energy, respectively. Since V_{ne}, V_{nn} and J are all electrostatic, they can be put together yielding the total electrostatic energy $E_e = V_{ne} + J + V_{nn}$ and thus we have $E = T_s + E_e + E_{xc}$. With this, we also have $E_q = T_s - E_s + E_{XC}$. For molecular systems in solvents, there is an extra term in the total energy partition coming from the contribution of the implicit solvent effect, E_{Solv}, so the above two total energy decomposition schemes in DFT will each have this term added. It should also be noted that steric energy in eqn (1) is only different from Fisher information[45,60–62] by a factor of 1/8 in the information-theoretic approach (ITA)[63–65] in DFT, which has been found to be closely related to Shannon entropy and other ITA quantities.[66–68] It should also be noted that eqn (1) has distinct physical meaning representing a hypothetical state and it satisfies homogeneous scaling properties.[38]

$$E = T_s + E_e + E_{xc} + E_{Solv} = E_s + E_e + E_q + E_{Solv}, \tag{2}$$

The density-based quantification of steric effects in eqn (1) is an explicit electron density functional. With its expression analytically known, steric energy can be augmented by following three physical concepts, (i) steric potential $\upsilon_s(r)$, which is defined as the functional derivative of the steric energy with respect to the electron density,[38]

$$\upsilon_s(r) = \frac{\delta E_s[\rho]}{\delta\rho(r)} = \frac{1}{8}\frac{|\nabla\rho(r)|^2}{\rho(r)} - \frac{1}{4}\frac{\nabla^2\rho(r)}{\rho(r)} \tag{3}$$

with $\nabla^2\rho$ as the Laplacian of the electron density; (ii) steric force $F_s(r)$,[52]

$$F_s(r) = -\nabla\cdot\upsilon_s(r) \tag{4}$$

and (iii) steric charge $q_s(r)$[51,69,70]

$$q_s(r) = -\frac{1}{4\pi}\nabla^2\upsilon_s(r) = -\frac{1}{4\pi}\nabla^2\left(\frac{\delta E_s[\rho]}{\delta\rho(r)}\right). \tag{5}$$

These quantities can be represented at molecular, group, and atomic levels using partition schemes such as Hirshfeld, Becke, and AIM (atoms-in-molecules).[26,71–73] The above set of formulae in eqn (1), (3), (4), and (5), steric energy, steric potential, steric force, and steric charge, forms our density-based approach to quantify the steric effect in DFT from the theoretical perspective.

From the experimental perspective, on the other hand, the steric effect has been previously quantified in the literature by the following acid-catalyzed hydrolysis of esters,[53,56,57,59,74]

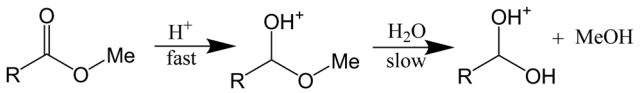

(6)

through the reaction rate of ester hydrolysis with a given substituent group R, k_s, in comparison with the rate of the reference hydrolysis with the methyl group R = CH_3, k_{CH_3},[53,56,57,59,74]

$$E_S = \frac{1}{\delta}\log\left(\frac{k_s}{k_{CH_3}}\right), \tag{7}$$

where E_S (capital letter S) is the Taft steric parameter, also known as Taft steric constants, which have been considered as the experimental scale in physical organic chemistry to quantify the steric effects of substituents on reaction rates and equilibria, and δ is a proportional constant describing the susceptibility of the reaction series to the effect. Taft's steric parameter (E_S) quantifies the steric effects generated by the substituent groups. The E_S values derived from the rates of ester hydrolysis reactions assume that the reaction center experiences different degrees of steric hindrance depending on the size of the substituent. E_S was determined relative to a reference compound, typically methyl (CH_3), which is assigned a value of zero. Larger substituents that cause greater steric hindrance have positive and larger E_S values, while smaller substituents that cause less steric hindrance have negative or smaller E_S values. For example, for the hydrogen group, $E_S = -1.12$, whereas for the *t*-butyl group, $E_S = 1.43$.[53] In this work, we correlate these two perspectives, one from the experiment and the other from theory, of quantifying the steric effect and validate our theoretical quantification by directly applying eqn (1) and (3)–(5) to the acid-catalyzed ester hydrolysis system in eqn (6) with different substituent R groups.

Before getting started, however, we have the following a few points in order. First, while these reaction rates in eqn (7), k_S

and k_{CH_3}, are experimentally accessible, computationally we approach the kinetic propensity of a reaction through its barrier height, which can be converted to the reaction rate through the Arrhenius equation if necessary. In this work, we directly use the barrier height for our purpose. Secondly, when hydrolysis is carried out in an acidic solvent, which can be simulated by the implicit solvent model in computation, multiple water molecules will explicitly participate in the reaction. It is impossible to computationally exhaust all combinations of different numbers of water molecules involved. Instead, we explore the mechanism using up to four water molecules and then ascertain the mechanism with the minimal number of water molecules required for the hydrolysis reaction to be effectively simulated.

Lastly, hydrolysis should proceed through a multiple-step mechanism, so the rates in eqn (7) are apparent reaction rates, not the ones from the rate-limiting step of the multi-step mechanism. We employ the energetic span model of Kozuch and Shaik[75,76] as the effective barrier height to account for the apparent reaction rate in eqn (7). The energetic span model is a conceptual framework used in catalysis theory to understand and predict the performance of catalytic cycles. It focuses on identifying and analyzing the key energetic parameters that govern the overall catalytic efficiency. An energetic span is defined as the difference in energy between the highest energy transition state and the lowest energy intermediate (including the reactant) along the reaction pathway. This span represents the overall energy barrier that must be overcome for the catalytic cycle to proceed.

Computational details

All calculations were performed with the Gaussian 16 package, version C01,[77] with ultrafine integration grids and tight self-consistent-field convergence. All molecular geometries were fully optimized first, and a single-point frequency calculation was followed to ensure that the final structure obtained has no imaginary frequency. We employed DFT functionals B3LYP and M06-2X and a few basis sets, such as Pople's standard triple-zeta split-valence basis set, 6-311+G(d), *etc.*, with and without dispersion correction for the calculation and benchmark purposes in this work. The solvent effect was considered by using the implicit solvent model of the CPCM (conductor polarizable continuum model) and SMD (solvation model based on density). The ''Multiwfn'' program version 3.8[78] was employed to calculate energetic components, steric effect quantities (steric energy, steric potential, steric force, and steric charge), and information-theoretic quantities, such as Shannon entropy, Fisher information, alternative Fisher information, Ghosh–Berkowitz–Parr entropy, information gain, relative Fisher information, alternative relative Fisher information, *etc.* They were performed by using the checkpoint file from the Gaussian calculations as the input file. Details of these information-theoretic quantities in definition and implementation are available elsewhere.[29,61,62,64,67,73,78–80] To consider the atomic contributions of these quantities, we employ the Hirshfeld scheme to partition atoms in molecules.[81] The total number of mesh points for the Hirshfeld numerical quadrature in the radial part and spherical surface is 300 and 3890, respectively.

Results and discussion

We first investigated the ester hydrolysis mechanism that can be employed for our study by changing the number of water molecules explicitly included in the reaction. For a mechanism to be feasible for our purpose, there is only one mandatory condition. That is, by increasing the size of the substituting group from H to methyl to *t*-butyl; for the rate-limiting step, the barrier height should be monotonically increased. This condition results from the very fact that this reaction has been employed to quantify the steric effect in the first place, so this condition must be true. The 3-step mechanism with multiple, $m + n$ in total, water molecules explicitly considered is shown in Scheme 1. The first step is the formation of the C–O bond between the carboxyl group and an incoming water molecule, the second step involves proton transfer, and the third step is the break of the ester C–O bond to complete hydrolysis. It has three transition state (TS) structures and two intermediates. Fig. 1 elucidates the hydrolysis mechanism with up to 4 water molecules explicitly included for esters, which are attached by three different substituting groups R with R = H, methyl, and *t*-butyl. Their optimized molecule coordinates are included in the ESI.† From the figure, it can be seen that (i) the rate-limiting step is TS2 for all three species and (ii) only 2- and 3-water mechanisms correctly reproduce the order of the steric effect for the three groups. This result suggests that we need at least two water molecules to reasonably simulate the hydrolysis process for esters. Also, we notice that the ''reactant'' in Fig. 1 was the starting molecule complex, as shown in Scheme 1, of the acid-catalyzed ester with multiple water molecules, which indeed is an intermediate from the perspective of the energetic span model. In this study, the energetic span is the difference of the total energy between TS2 and the reactant in Scheme 1.

Can the result obtained in Fig. 1 be extended to groups other than alkyl groups, such as aromatic groups or strongly electronegative ones? Fig. 2 illustrates the comparison of the hydrolysis mechanism with F and Ph_3C groups together with that of the *t*-butyl group. For F and Ph_3C groups, the rate-limiting step is changed to TS3, but for the alkyl group, we know from Fig. 1, it is TS2. This difference in the mechanism suggests that different functional groups can result in different rate-limiting steps, so they do not belong to the same category from the mechanism viewpoint. For this reason, we only consider alkyl groups in this study.

Table 1 summarizes the effective barrier height results for the 2-water reaction mechanism obtained from five different methodologies for 20 alkyl groups in solvent water. Their corresponding Taft steric parameters E_S from the literature[53] are also tabulated in the table. The last row is the correlation

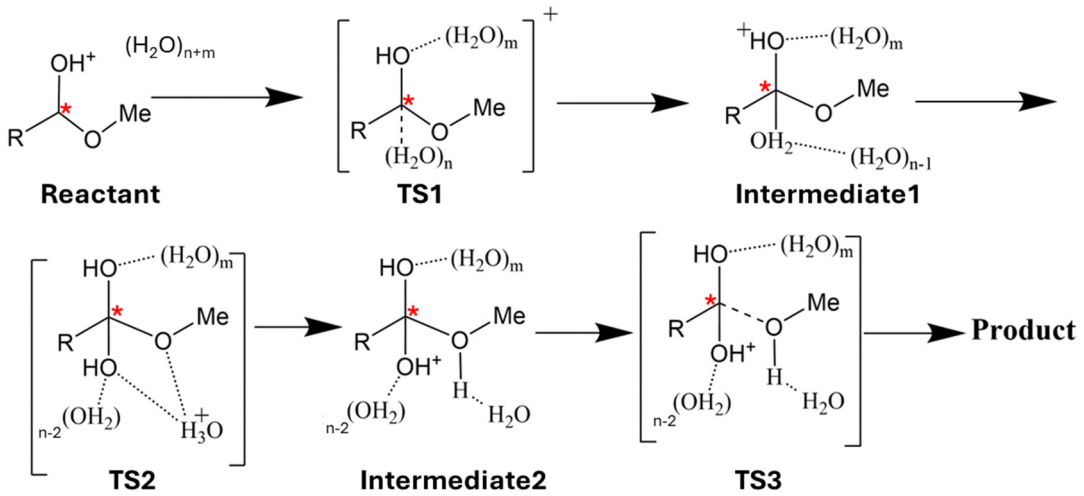

Scheme 1 The 3-step reaction mechanism of acid-catalyzed ester hydrolysis in water solvent with (n + m) water molecules explicitly included. The starting system is the molecular complex of the protonated ester with (n + m) water molecules. The central carbon atom marked by a star (*) symbol serves as the reaction center.

coefficient R^2 value between Taft steric parameters and calculated barrier heights for the 20 alkyl groups. As an illustrative example, Fig. 3a exhibits the strong correlation of Taft steric parameters with the barrier height results from the M06-2X/6-311++G(d,p) level of theory in water solvent using the SMD implicit solvent model. As can be seen from the table and Fig. 3a, (i) the correlations between Taft steric parameters and barrier heights are markedly strong across all five different methods that we examined in this work, all with R^2 better than 0.93, suggesting that the 2-water reaction mechanism in Fig. 1 is a valid and reliable representation of the acid-catalyzed hydrolysis of esters with alkyl groups; and (ii) the choice of methodologies does significantly impact the barrier height values, especially when different exchange–correlation functionals are employed. We considered other methodologies as well, including MP2 (not shown). No matter what methodologies are employed, the correlation between Taft steric parameters and barrier heights is always strong, confirming the validity and robustness of the correlation and independence of our results on functionals and basis sets.

With the hydrolysis mechanism computationally established, we are ready to answer the question that we posed earlier. That is, is there any correlation between the theoretical quantification of steric effect and the Taft steric parameter obtained from experiment? The correlation between the barrier height of 20 systems studied in this work and the difference of steric energy, eqn (1), on the central carbon atom with the correlation coefficient R^2 = 0.929 is shown in Fig. 3b. The difference of steric

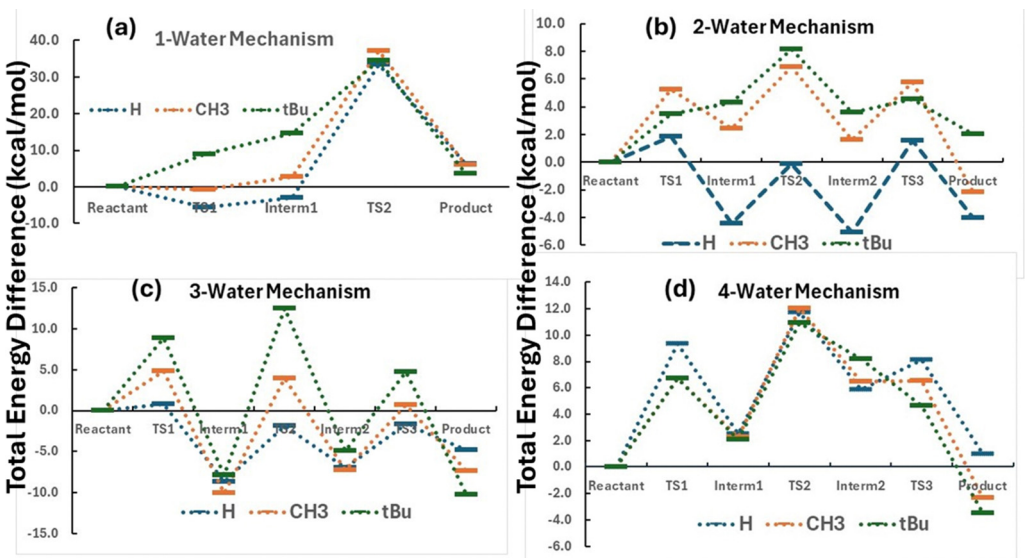

Fig. 1 Acid-catalyzed ester hydrolysis mechanisms of different groups (R = H, CH_3, and tBu) with (a) one (m = 0 and n = 1), (b) two (m = 0 and n = 2), (c) three (m = 0 and n = 3), and (d) four (m = 1 and n = 3) water molecules explicitly included in Scheme 1.

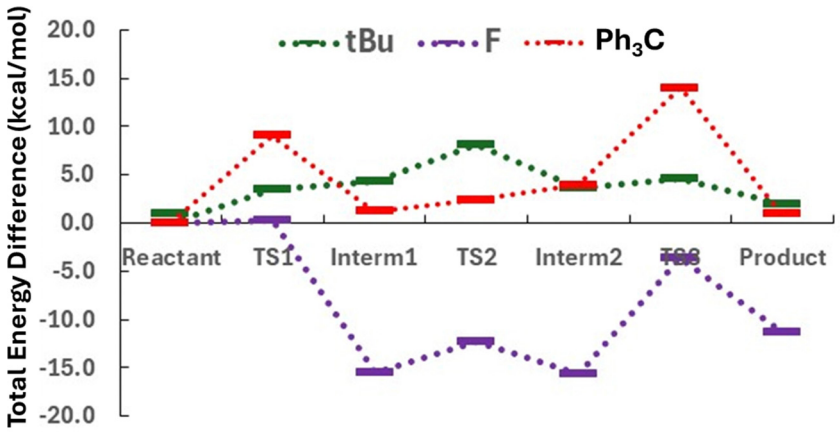

Fig. 2 The 2-water acid-catalyzed ester hydrolysis mechanism with three R groups (R = *t*Bu, F, and Ph_3C) of vastly different (alkly, aromatic, and strongly electronegative) groups in Scheme 1.

Table 1 The hydrolysis barrier height for the 2-water reaction mechanism obtained by five different methodologies for 20 alkyl R groups in Scheme 1 in solvent water. Their corresponding Taft steric parameters are also tabulated. The last row shows the correlation coefficients R^2 between Taft steric parameters and calculated barrier heights. Barrier heights in kcal mol^{-1}

Alkyl group–R	Taft E_S	Method 1	Method 2	Method 3	Method 4	Method 5
C_2H_5	0.08	7.51	7.49	5.44	14.70	7.45
C_3H_7	0.36	7.51	7.48	5.43	14.78	7.32
C_4H_9	0.39	7.57	7.54	5.48	14.87	7.38
CH_3	0.00	7.00	7.00	4.85	14.15	6.86
Cyclohexane	0.69	8.21	8.16	6.03	15.91	7.53
Et_2CH	2.00	12.82	12.82	10.74	18.87	12.73
$EtMe_2C$	2.28	11.83	11.81	9.74	19.85	11.59
H	−1.12	0.41	0.39	−1.58	6.82	0.28
iBut	0.93	9.08	9.01	6.21	17.35	7.54
iPrEtCH	3.23	15.44	15.42	13.35	23.90	16.60
iPr	0.47	7.56	7.56	5.68	15.29	6.96
Pr_2CH	2.03	12.84	12.85	10.80	18.98	12.78
PrEtCH	2.00	12.27	12.22	9.81	18.77	11.02
PrMeCH	1.02	9.37	9.34	7.15	17.14	8.90
sBut	1.00	9.40	9.39	7.35	16.60	9.25
$tBuCH_2Me_2C$	2.48	12.29	12.25	10.04	20.89	12.64
$tBuCH_2MeCH$	1.81	12.05	11.86	9.79	17.88	11.11
$tBuCH_2$	1.63	11.05	10.96	8.79	18.71	10.46
*t*BuMeCH	3.21	15.86	15.86	13.63	23.49	15.68
*t*Bu	1.43	10.35	9.87	7.78	17.77	9.70
R^2		0.947	0.946	0.944	0.935	0.942

Taft steric parameters are from ref. 53. All methods employed the SMD implicit solvent model. Method 1 is at the M06-2X/6-311++G(d,p) level of theory; method 2 is at M062X/6-311++G(d,p) with the GD3 dispersion correction; method 3 is at M062X/6-311+G(d) with the GD3 dispersion correction; method 4 is same as method 2 except that M062X was replaced by B3LYP; method 5 is same as method 2 except that a larger basis set, aug-cc-pVDZ, was utilized.

energy is between TS2 and the reactant, same as the barrier height defined by the energetic span model.[75,76] When the Taft steric parameter and the steric energy difference on the central carbon are directly correlated, we obtain the correlation coefficient R^2 = 0.904. These results indicate that the answer to the above question is positive and decisively favorable. We obtained a strong correlation between theoretical and experimental quantifications of steric effects.

Moreover, we correlate the barrier height results with the three other physical variables from the scheme of our quantification, steric potential, steric force, and steric charge, defined in eqn (3)–(5), respectively. Fig. 4 shows the result of these additional correlations for the central carbon atom. From the figure, we can see that steric potential and steric charge are positively correlated with the barrier height, whereas the magnitude of the steric force is negatively correlated. Even though the correlation with the steric force is the least strong (with R^2 = 0.83), the one with steric potential and steric charge is significantly stronger, with R^2 = 0.92 and 0.95, respectively. When Taft steric parameters are directly correlated with the steric charge, we obtained R^2 = 0.94. These results confirm what we have obtained in Fig. 3b, suggesting that experimental and

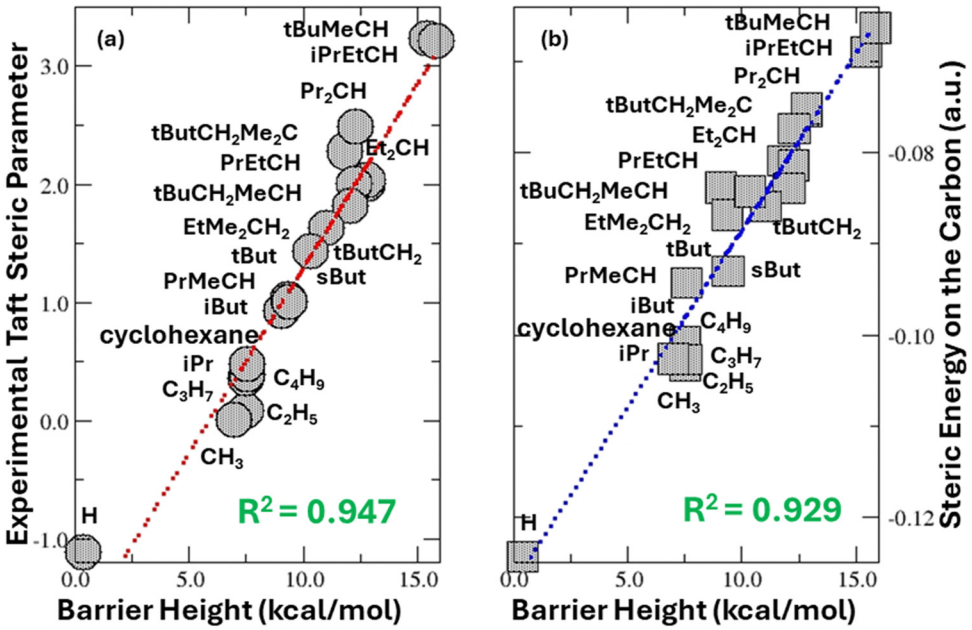

Fig. 3 Strong linear correlations of the 2-water hydrolysis barrier height from method 1 with (a) experimental Taft parameters and (b) the difference of the steric energy between TS2 and the reactant in the 2-water hydrolysis mechanism in Fig. 2 on the central carbon atom for 20 alkyl groups.

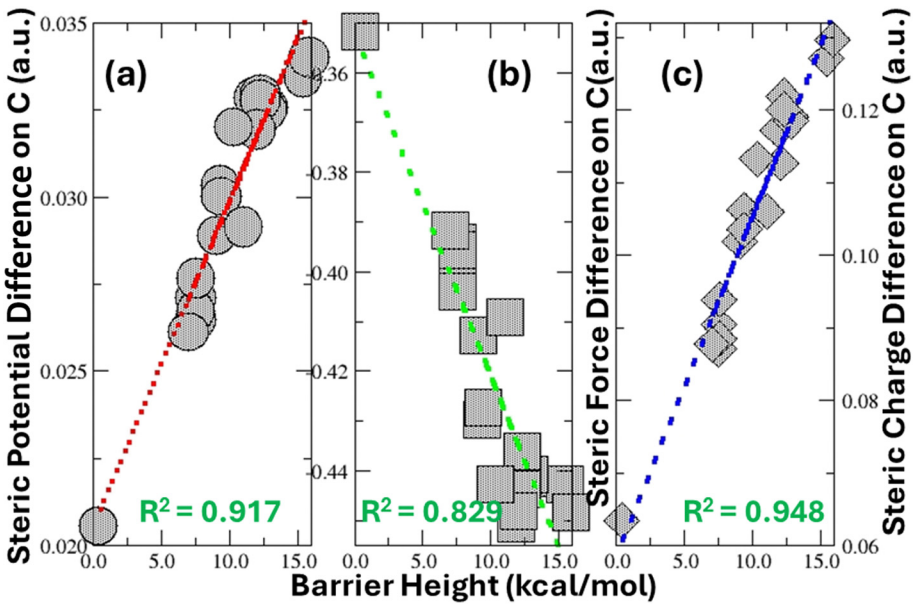

Fig. 4 Strong linear correlations of the barrier height with the difference of the (a) steric potential, (b) magnitude of the steric force, and (c) steric charge between TS2 and the reactant in the 2-water hydrolysis mechanism in Fig. 2 on the central carbon atom for 20 alkyl groups.

theoretical quantifications of steric effects are strongly correlated. Put together, these results from steric energy, steric potential, steric force, and steric charge validate the effectiveness of our theoretical approach to formulate and quantify the steric effect using density-based quantities.

We employed the steric propensities on the central carbon atom in Scheme 1 to correlate with Taft steric parameters in Fig. 3b and 4. There is a reason for this. No matter what substituent groups R are replaced in eqn (6), their impact on the reactivity of hydrolysis should eventually be passed to the central carbon atom, which is the reaction center, and thus reflected by the change of its properties. In this regard, it makes sense that we utilize different steric-related propensities of the central carbon atom for the correlation purpose. However, can we still use the results from the molecular level to do that? Using the difference at the molecular level between TS2 and the

Table 2 The decomposition results for the hydrolysis barrier height of the 2-water reaction mechanism using method 1 for 20 alkyl groups in Scheme 1 in solvent water using the two total energy partition schemes in DFT. Units in kcal mol^{-1}

Alkyl group–R	ΔE	ΔE_{Solv}	ΔT_s	ΔE_{xc}	ΔE_e	ΔE_s	ΔE_q
C_2H_5	**7.51**	**−5.27**	**−37.47**	**−16.69**	**66.94**	**300.04**	**−354.20**
C_3H_7	**7.51**	**−6.80**	**−34.69**	**−17.26**	**66.26**	**307.45**	**−359.41**
C_4H_9	**7.57**	**−6.75**	**−35.60**	**−17.13**	**67.04**	**306.52**	**−359.25**
CH_3	**7.00**	**−4.45**	**−37.31**	**−16.77**	**65.52**	**306.17**	**−360.24**
Cyclohexane	**8.21**	**−4.16**	**−41.30**	**−18.69**	**72.35**	**350.41**	**−410.40**
Et_2CH	**12.82**	**−0.16**	**−37.71**	**−19.25**	**69.94**	**347.83**	**−404.79**
$EtMe_2C$	**11.83**	**−3.26**	**−40.07**	**−19.61**	**74.77**	**353.16**	**−412.84**
H	**0.41**	**−3.74**	**−32.06**	**−16.57**	**52.78**	**296.53**	**−345.16**
iBut	**9.08**	**−3.39**	**−41.19**	**−18.99**	**72.65**	**354.73**	**−414.92**
iPrEtCH	**15.44**	**−1.63**	**−43.47**	**−18.17**	**78.71**	**329.32**	**−390.96**
iPr	**7.56**	**−6.91**	**−45.58**	**−17.62**	**77.68**	**333.90**	**−397.10**
Pr_2CH	**12.84**	**−0.44**	**−36.68**	**−19.43**	**69.39**	**350.64**	**−406.75**
PrEtCH	**12.27**	**−0.93**	**−34.08**	**−21.68**	**68.97**	**377.29**	**−433.06**
PrMeCH	**9.37**	**−4.04**	**−45.49**	**−19.03**	**77.92**	**357.23**	**−421.76**
sBut	**9.40**	**−3.30**	**−37.95**	**−18.58**	**69.23**	**342.47**	**−399.01**
tBuCH$_2$Me$_2$C	**12.29**	**−8.14**	**−45.83**	**−18.99**	**85.26**	**341.92**	**−406.75**
tBuCH$_2$MeCH	**12.05**	**−10.58**	**−47.16**	**−18.80**	**88.59**	**350.86**	**−416.82**
tBuCH$_2$	**11.05**	**−5.97**	**−37.97**	**−18.86**	**73.84**	**340.76**	**−397.58**
tBuMeCH	**15.86**	**−1.88**	**−43.20**	**−18.21**	**79.15**	**328.40**	**−389.80**
tBu	**10.35**	**−5.68**	**−45.30**	**−18.40**	**79.73**	**346.35**	**−410.05**

reactant, even though the correlation with steric energy and steric force is less strong, the correlation with steric potential (R^2 = 0.87) and steric charge (R^2 = 0.91) is still considerably significant. In this regard, our answer to the above question is still favorable.

Let us now examine the results from the two total energy partition schemes in DFT, eqn (2), for these systems. Table 2 shows the decomposition results for the hydrolysis barrier height of the 2-water reaction mechanism for 20 alkyl groups at the M062X/6-311++G(d,p) level of theory in solvent water using the SMD implicit solvent model. From the table, we can see that (i) with the conventional DFT partition scheme, $\Delta E = \Delta E_{Solv} + \Delta T_s + \Delta E_e + \Delta E_{xc}$, the only positive and thus dominant contributor to ΔE is from the electrostatic component ΔE_e, and all other three terms contribute negatively. This is the same as what we previously observed for other systems,[39–41,45–47,50,82]

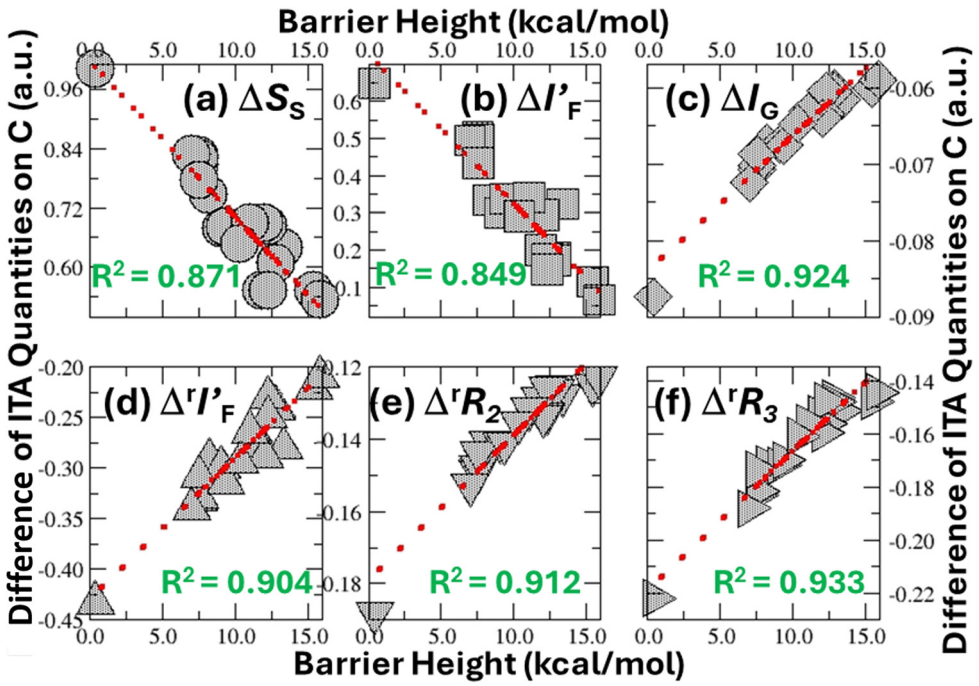

Fig. 5 Strong linear correlations of the 2-water hydrolysis barrier height with the difference of (a) Shannon entropy, (b) alternative Fisher information, (c) information gain, (d) relative alternative Fisher information, (e) second-order relative Rényi entropy, and (f) third-order relative Rényi entropy from the information-theoretic approach in DFT between TS2 and the reactant of the 2-water hydrolysis mechanism in Fig. 2 on the central carbon atom for 20 alkyl groups.

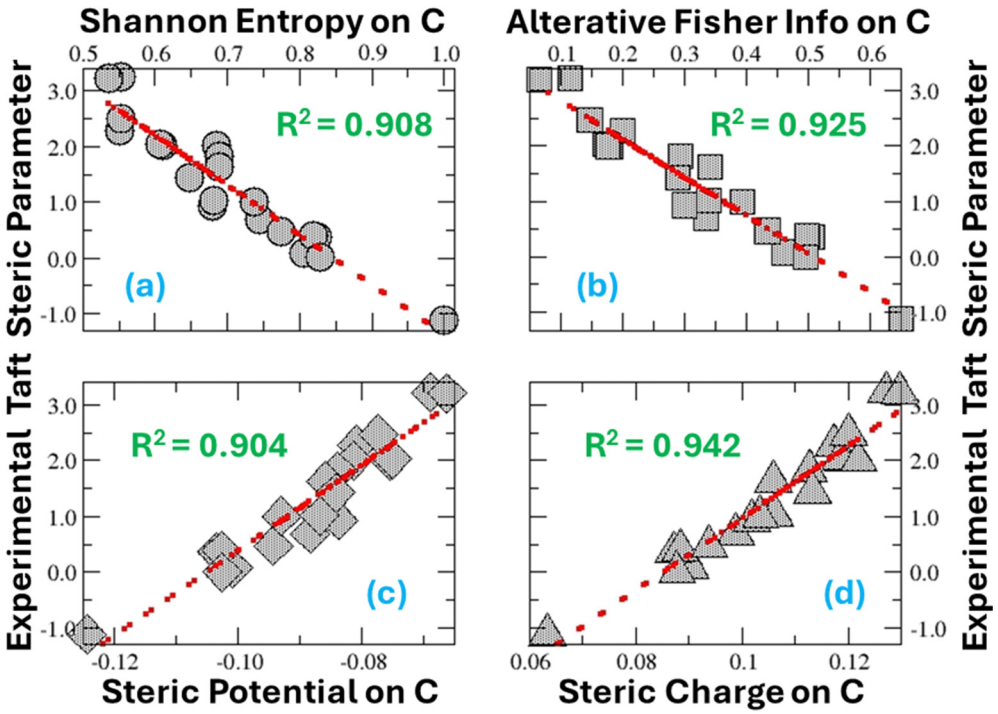

Fig. 6 Strong linear relationships between the Taft steric parameter of 20 systems studied in this work and the atomic difference of (a) Shannon entropy, (b) alternative Fisher information, (c) steric potential, and (d) steric charge on the reaction center. The difference was taken between TS2 and the reactant of the 2-water hydrolysis mechanism in Fig. 2 on the central carbon atom for 20 alkyl groups using the Hirshfeld partition.

However, different from the previous systems, the correlation between ΔE_e and ΔE is not significant (with R^2 = 0.467 only). (ii) With the second partition scheme, $\Delta E = \Delta E_{Solv} + \Delta E_s + \Delta E_e + \Delta E_q$, both ΔE_e and ΔE_s contribute positively but the magnitude of ΔE_s is much larger than that of ΔE_e, suggesting that the barrier height is dominated by the steric effect. Nevertheless, no strong correlation at the molecular level is obtained for ΔE with any of these two components. Using multivariant fittings, however, same as what we did previously,[39,47,50,82] better correlations can be obtained from both partition schemes. For example, with ΔE_{Solv}, ΔE_e, and ΔE_s, we have R^2 = 0.822, and with ΔE_{Solv}, ΔE_e, and ΔE_{xc}, we obtain R^2 = 0.811 (not shown). These results are the same as the other systems that we previously investigated.[39–41,45–47,50,82]

Since steric energy differs from Fisher information only by a factor of 1/8, and the latter was proven to be intrinsically related[67,83] to other quantities from the information-theoretic approach (ITA),[63–65] we next examine correlations of the barrier height with ITA quantities. Strong correlations of the barrier height with the difference of six ITA quantities, including Shannon entropy ΔS_S, alternative Fisher information $\Delta I'_F$, information gain ΔI_G, relative alternative Fisher information $\Delta^r I'_F$, second-order relative Rényi entropy $\Delta^r R^2$, and third-order relative Rényi entropy $\Delta^r R_3$, are shown in Fig. 5. The difference of these ITA quantities was taken between TS2 and the reactant of the 2-water hydrolysis mechanism in Fig. 2 on the central carbon atom for 20 alkyl groups. As can be seen from the figure, all these six ITA quantities are strongly correlated with the barrier height of ester hydrolysis for 20 alkyl groups. These results not only verify the intrinsic relationship among ITA quantities, but also suggest that we could have more quantitative descriptors for Taft steric parameters.

Finally, as a further piece of evidence, as shown in Fig. 6, we directly correlated Taft steric parameters with the descriptors from both steric quantifications (steric potential and steric charge) and ITA quantities (Shannon entropy and alternative Fisher information) on the carbon center. From the figure, we can see all four descriptors generated significantly strong correlations with Taft constants, all with the correlation coefficient larger than 0.90. These results confirm, again, the effectiveness and validity of employing the DFT scheme and ITA quantities to quantitatively describe the steric effect.

Conclusions

To summarize, in this work, we applied the theoretical quantification scheme from density functional theory for the acid catalyzed hydrolysis of esters with 20 different substituent groups, whose experimental scale of Taft steric parameters was previously established in the literature. The main results from this work are as follows. Firstly, a computational model to effectively simulate the hydrolysis mechanism in acidic solvents is established. At least two water molecules must be explicitly considered. Secondly, to represent the effective barrier height of the multi-step mechanism for ester hydrolysis and to correlate it with the apparent reaction rate from experimental measurements, the energetic span model from the literature must be employed. Thirdly, we observed strong

correlations of the barrier height with Taft steric parameters and with the four steric effect related variables, including steric energy, steric potential, steric force, and steric charge. Lastly, we obtained strong correlations of the barrier height with six different information-theoretic quantities. These results provide pieces of strong evidence in support that the density-based quantification of steric effects using Weizsäcker kinetic energy and its derivatives is a valid and robust one, and that steric effects can be quantitatively described and well accounted for by numerous density-based quantities in the framework of density functional theory. It is our humble view that this work should have satisfactorily addressed the issue of how the steric effect can be formulated in such a way that a direct comparison with experiments is made possible. It is our hope that this work might have laid the groundwork for future applications, where both steric, electrostatic, and quantum can be quantitatively accounted for.

Data availability

Cartesian coordinates of optimized reactants and transition state structures are included in ESI.† The data that support the findings of this study are available from the corresponding author, SL, upon reasonable request.

Conflicts of interest

There are no conflicts to declare.

Acknowledgements

C. Y. R. acknowledges support from the National Natural Science Foundation of China (Grant No. 22373034) and the Hunan Province College Students Research Learning and Innovative Experiment project (S202310542078). D. B. Z. is supported by the start-up funding of Yunnan University, the Yunnan Fundamental Research Projects (Grant No. 202101AU070012). A part of the computations were performed using the high-performance computers of the Advanced Computing Center of Yunnan University.

References

1 R. G. Parr and W. T. Yang, *Density-functional theory of atoms and molecules*, Oxford University Press, New York, 1989.
2 A. M. Teale, T. Helgaker, A. Savin, C. Adamo, B. Aradi, A. V. Arbuznikov, P. W. Ayers, E. J. Baerends, V. Barone and P. Calaminici, *et al.*, *Phys. Chem. Chem. Phys.*, 2022, **24**, 28700–28781.
3 C. Y. Rong, D. B. Zhao, X. He and S. B. Liu, *J. Phys. Chem. Lett.*, 2022, **13**, 11191–11200.
4 X. He, M. Li, C. Y. Rong, D. B. Zhao, W. J. Liu, P. W. Ayers and S. B. Liu, *J. Phys. Chem. A*, 2024, **128**, 1183–1196.
5 R. G. Parr and W. T. Yang, *Annu. Rev. Phys. Chem.*, 1995, **46**, 701–728.
6 P. Geerlings, F. De Proft and W. Langenaeker, *Chem. Rev.*, 2003, **103**, 1793–1873.
7 P. Geerlings, E. Chamorro, P. K. Chattaraj, F. De Proft, J. L. Gázquez, S. B. Liu, C. Morell, A. Toro-Labbé, A. Vela and P. W. Ayers, *Theor. Chem. Acc.*, 2020, **139**, 36.
8 S. B. Liu, *Acta Phys. Chim. Sin.*, 2009, **25**, 590–600.
9 S. B. Liu, *Conceptual Density Functional Theory: Towards a New Chemical Reactivity Theory*, Wiley-VCH, Germany, 2022.
10 P. K. Chattaraj and P. W. Ayers, *J. Chem. Phys.*, 2005, **123**, 086101.
11 R. G. Pearson, *Acc. Chem. Res.*, 1993, **26**, 250–255.
12 R. G. Parr and R. G. Pearson, *J. Am. Chem. Soc.*, 1983, **105**, 7512–7516.
13 W. T. Yang and R. G. Parr, *Proc. Natl. Acad. Sci. U. S. A.*, 1985, **82**, 6723–6726.
14 T. L. Li, S. B. Liu, S. X. Feng and C. E. Aubrey, *J. Am. Chem. Soc.*, 2005, **127**, 1364–1365.
15 W. T. Yang, R. G. Parr and R. Pucci, *J. Chem. Phys.*, 1984, **81**, 2862–2863.
16 P. K. Chattaraj, U. Sarkar and D. R. Roy, *Chem. Rev.*, 2006, **106**, 2065–2091.
17 R. G. Parr, L. v Szentpály and S. B. Liu, *J. Am. Chem. Soc.*, 1999, **121**, 1922–1924.
18 A. D. Becke and K. E. Edgecombe, *J. Am. Chem. Soc.*, 1990, **92**, 5397–5403.
19 B. Silvi and A. Savin, *Nature*, 1994, **371**, 683–686.
20 A. Savin, R. Nesper, S. Wengert and T. F. Fässler, *Angew. Chem., Int. Ed. Engl.*, 1997, **36**, 1808–1832.
21 E. R. Johnson, S. Keinan, P. Mori-Sánchez, J. Contreras-García, A. J. Cohen and W. T. Yang, *J. Am. Chem. Soc.*, 2010, **132**, 6498–6506.
22 J. Contreras-García, E. R. Johnson, S. Keinan, R. Chaudret, J.-P. Piquemal, D. N. Beratan and W. T. Yang, *J. Chem. Theory Comput.*, 2011, **7**, 625–632.
23 S. Liu, C. Rong, T. Lu and H. Hu, *J. Phys. Chem. A*, 2018, **122**, 3087–3095.
24 Y. Huang, L. Liu, C. Rong, T. Lu, P. W. Ayers and S. Liu, *J. Mol. Model.*, 2018, **24**, 213.
25 S. J. Zhong, X. He, S. Y. Liu, B. Wang, T. Lu, C. Y. Rong and S. B. Liu, *J. Phys. Chem. A*, 2022, **126**, 2437–2444.
26 S. B. Liu, C. Y. Rong and T. Lu, *J. Phys. Chem. A*, 2014, **118**, 3698–3704.
27 B. Wang, C. Y. Rong, P. K. Chattaraj and S. B. Liu, *Theor. Chem. Acc.*, 2019, **138**, 124.
28 S. B. Liu, *J. Phys. Chem. A*, 2015, **119**, 3107–3111.
29 S. B. Liu, *J. Chem. Phys.*, 2014, **141**, 194109.
30 C. Y. Rong, D. B. Zhao, T. J. Zhou, S. Y. Liu, D. H. Yu and S. B. Liu, *J. Phys. Chem. Lett.*, 2019, **10**, 1716–1721.
31 C. Y. Rong, D. B. Zhao, D. H. Yu and S. B. Liu, *Phys. Chem. Chem. Phys.*, 2018, **20**, 17990–17998.
32 J. Nochebuena, J.-P. Piquemal, S. Liu and G. A. Cisneros, *J. Chem. Theory Comput.*, 2023, **19**, 7715–7730.
33 S. B. Liu and C. Y. Rong, *J. Phys. Chem. A*, 2021, **125**, 4910–4917.
34 M. Li, X. He, J. Chen, B. Wang, S. B. Liu and C. Y. Rong, *J. Phys. Chem. A*, 2021, **125**, 1269–1278.

35 S. B. Liu, *J. Phys. Chem. Lett.*, 2020, **11**, 8690–8696.
36 S. B. Liu, *J. Phys. Chem. Lett.*, 2021, **12**, 8720–8725.
37 R. F. W. Bader, *Atoms in Molecules*, Oxford University Press, 1989.
38 S. B. Liu, *J. Chem. Phys.*, 2007, **126**, 244103.
39 Y. Huang, A. G. Zhong, Q. Yang and S. B. Liu, *J. Chem. Phys.*, 2011, **134**, 084103.
40 S. B. Liu, H. Hu and L. G. Pedersen, *J. Phys. Chem. A*, 2010, **114**, 5913–5918.
41 D. H. Ess, S. B. Liu and F. De Proft, *J. Phys. Chem. A*, 2010, **114**, 12952–12957.
42 M. Torrent-Sucarrat, S. B. Liu and F. De Proft, *J. Phys. Chem. A*, 2009, **113**, 3698–3702.
43 V. G. Tsirelson, A. I. Stash and S. B. Liu, *J. Chem. Phys.*, 2010, **133**, 114110.
44 D. Fang, J.-P. Piquemal, S. B. Liu and G. A. Cisneros, *Theor. Chem. Acc.*, 2014, **133**, 1484.
45 R. O. Esquivel, S. B. Liu, J. C. Angulo, J. S. Dehesa, J. Antolín and M. Molina-Espíritu, *J. Phys. Chem. A*, 2011, **115**, 4406–4415.
46 S. B. Liu and N. Govind, *J. Phys. Chem. A*, 2008, **112**, 6690–6699.
47 S. B. Liu, *J. Phys. Chem. A*, 2013, **117**, 962–965.
48 X. F. Cao, S. Y. Liu, C. Y. Rong, T. Lu and S. B. Liu, *Chem. Phys. Lett.*, 2017, **687**, 131–137.
49 X. Zhou, D. H. Yu, C. Y. Rong, T. Lu and S. B. Liu, *Chem. Phys. Lett.*, 2017, **684**, 97–102.
50 Z. Wu, C. Y. Rong, T. Lu, P. W. Ayers and S. B. Liu, *Phys. Chem. Chem. Phys.*, 2015, **17**, 27052–27061.
51 S. B. Liu, L. H. Liu, D. H. Yu, C. Y. Rong and T. Lu, *Phys. Chem. Chem. Phys.*, 2018, **20**, 1408–1420.
52 S. B. Liu, C. Y. Rong and T. Lu, *Phys. Chem. Chem. Phys.*, 2017, **19**, 1496–1503.
53 J. A. MacPhee, A. Panaye and J.-E. Dubois, *Tetrahedron*, 1978, **34**, 3553–3562.
54 B. Bumbăcilă and M. V. Putz, New Frontiers in Nanochemistry: Concepts, *Theories, and Trends*, Apple Academic Press, 2020.
55 B. Pinter, T. Fievez, F. M. Bickelhaupt, P. Geerlings and F. De Proft, *Phys. Chem. Chem. Phys.*, 2012, **14**, 9846–9854.
56 R. W. Taft, *J. Am. Chem. Soc.*, 1952, **74**, 3120–3128.
57 R. W. Taft, *J. Am. Chem. Soc.*, 1953, **75**, 4538–4539.
58 M. Charton, *J. Org. Chem.*, 1978, **43**, 3995–4001.
59 M. Charton, *J. Am. Chem. Soc.*, 1975, **97**, 1552–1556.
60 Á. Nagy, *Int. J. Quantum Chem.*, 2022, **122**, e26679.
61 B. Wang, D. B. Zhao, T. Lu, S. B. Liu and C. Y. Rong, *J. Phys. Chem. A*, 2021, **125**, 3802–3811.
62 R. A. Fisher, *Math. Proc. Camb. Phil. Soc.*, 1925, **22**, 700–725.
63 C. Y. Rong, B. Wang, D. B. Zhao and S. B. Liu, *WIREs Comput. Mol. Sci.*, 2020, **10**, e1461.
64 S. B. Liu, *Acta Phys. Chim. Sin.*, 2016, **32**, 98–118.
65 X. Y. Zhou, C. Y. Rong, T. Lu, P. P. Zhou and S. B. Liu, *J. Phys. Chem. A*, 2016, **120**, 3634–3642.
66 S. B. Liu, *J. Chem. Phys.*, 2022, **157**, 101103.
67 S. B. Liu, *J. Chem. Phys.*, 2007, **126**, 191107.
68 X. He, T. Lu, C. Y. Rong, S. B. Liu, P. W. Ayers and W. J. Liu, *J. Chem. Phys.*, 2023, **159**, 054112.
69 S. B. Liu, P. W. Ayers and R. G. Parr, *J. Chem. Phys.*, 1999, **111**, 6197–6203.
70 G. Menconi, D. J. Tozer and S. B. Liu, *Phys. Chem. Chem. Phys.*, 2000, **2**, 3739–3742.
71 F. Heidar-Zadeh, P. W. Ayers, T. Verstraelen, I. Vinogradov, E. Vöhringer-Martinez and P. Bultinck, *J. Phys. Chem. A*, 2018, **122**, 4219–4245.
72 R. F. Nalewajski and R. G. Parr, *Proc. Natl. Acad. Sci. U. S. A.*, 2000, **97**, 8879–8882.
73 C. Y. Rong, T. Lu, P. K. Chattaraj and S. B. Liu, *Indian. J. Chem. Sect. A*, 2014, **53**, 970–977.
74 R. W. Taft, *J. Am. Chem. Soc.*, 1952, **74**, 2729–2732.
75 S. Kozuch, *WIREs Comput. Mol. Sci.*, 2012, **2**, 795–815.
76 S. Kozuch and S. Shaik, *Acc. Chem. Res.*, 2011, **44**, 101–110.
77 M. J. Frisch, G. W. Trucks, H. B. Schlegel, G. E. Scuseria, M. A. Robb, J. R. Cheeseman, G. Scalmani, V. Barone, G. A. Petersson, H. Nakat-suji, X. Li, M. Caricato, A. V. Marenich, J. Bloino, B. G. Janesko, R. Gomperts, B. Mennucci, H. P. Hratchian, J. V. Ortiz, A. F. Izmaylov, J. L. Sonnenberg, D. Williams-Young, F. L. F. Ding, F. Egidi, J. Goings, B. Peng, A. Petrone, T. Henderson, D. Ranasinghe, V. G. Zakrzewski, J. Gao, N. Rega, G. Zheng, W. Liang, M. Hada, M. Ehara, K. Toyota, R. Fukuda, J. Hasegawa, M. Ishida, T. Nakajima, Y. Honda, O. Kitao, H. Nakai, T. Vreven, K. Throssell, J. A. Montgomery, J. E. Peralta, F. Ogliaro, M. J. Bearpark, J. J. Heyd, E. N. Brothers, K. N. Kudin, V. N. Staroverov, T. A. Keith, R. Kobayashi, J. Normand, K. Raghavachari, A. P. Rendell, J. C. Burant, S. S. Iyengar, J. Tomasi, M. Cossi, J. M. Millam, M. Klene, C. Adamo, R. Cammi, J. W. Ochterski, R. L. Martin, K. Morokuma, O. Farkas and J. B. Foresman, *Gaussian16, Revision C.01*, Gaussian, Inc., Wallingford CT, 2016.
78 T. Lu and F. W. Chen, *J. Comput. Chem.*, 2012, **33**, 580–592.
79 C. E. Shannon, *Bell Syst. Tech. J.*, 1948, **27**, 3–55.
80 S. B. Liu, C. Y. Rong, Z. M. Wu and T. Lu, *Acta Phys. Chim. Sin.*, 2015, **31**, 2057–2063.
81 F. L. Hirshfeld, *Theor. Chem. Acc.*, 1977, **44**, 129–138.
82 S. B. Liu and C. K. Schauer, *J. Chem. Phys.*, 2015, **142**, 054107.
83 S. B. Liu, *J. Chem. Phys.*, 2019, **151**, 141103.

